Angular Dependence of Low-Energy Electron-Impact Excitation Cross Section of the Lowest Triplet States of H_2

S. TRAJMAR,* D. C. CARTWRIGHT,†,‡ J. K. RICE,† R. T. BRINKMANN,* AND A. KUPPERMANN†

California Institute of Technology, Pasadena, California

(Received 12 July 1968)

The differential cross sections for the electron-impact excitation of the lowest triplet states of molecular hydrogen ($b\ ^3\Sigma_u^+$, $a\ ^3\Sigma_g^+$) have been calculated from threshold to 85 eV impact energy using the Ochkur–Rudge theory. For the $X\ ^1\Sigma_g^+ \rightarrow b\ ^3\Sigma_u^+$ transition, the relative differential cross sections were measured with a low-energy, high-resolution electron-impact spectrometer from 10° to 80° scattering angle and impact energies of 25, 35, 40, 50, and 60 eV. Theory and experiment are in good agreement for the shape of the differential cross section for energies of 35 eV and above. However, at 25 eV, the theory continues to predict a rather well-developed maximum in the cross section at around 40° while the experimental cross sections are more isotropic. An appreciable contribution to the inelastic scattering in the energy loss region from 11 to 14 eV due to excitation to the $a\ ^3\Sigma_g^+$ and/or $c\ ^3\Pi_u$ states is definitely established from the observed angular distributions. A quantitative evaluation of the individual angular behavior of the excitations in this region, however, would require a resolution higher than the presently available one of 0.030 eV.

I. INTRODUCTION

Low-energy electron-impact spectroscopy has been found to be a very powerful tool for locating and identifying energy levels of molecules, especially those to which transitions from the ground state are forbidden by optical selection rules.[1–9] (The low-energy range as defined here is from a few electron volts up to 100 eV. This corresponds to the binding energy of outer electrons in atoms and molecules and is a very important region from the point of view of spectroscopy, photochemistry, plasma physics, and study of many atmospheric phenomena.) Both the energy and angular dependences of the differential cross section are important in identifying a given transition. The energy dependence of the differential cross section has been investigated to some degree in the past.[1–9] However, there is very little information available on the angular dependence of excitation cross sections at low impact energies. The Born–Oppenheimer approximation is not valid at these impact energies; in fact, no theory has proved reliable in predicting the energy and angular dependences of differential cross sections for even the simplest system of electron–atomic hydrogen.

Recent studies of He,[9a] C_2H_2,[9b] H_2, N_2, CO, CO_2, H_2O, and C_2H_4,[10] indicate that the measurement of the differential cross section at a fixed incident energy and variable scattering angle yields more information about the nature of the electronic excitation than does the measurement of the energy dependence of the differential cross section at a fixed scattering angle. In order to learn more about the angular behavior of differential cross sections for different types of electronic excitations, it is important to carry out experiments on transitions of known character. The information obtained from such studies is useful in the evaluation of different approximate theories and may lead to rules for assigning unknown transitions.

The hydrogen molecule, being the molecule most amenable to theoretical calculation, was the natural selection for comparison between theory and experiment. Cartwright and Kuppermann[11] have calculated total cross sections for the electron-impact excitation of the two lowest triplet states of molecular hydrogen using the Ochkur–Rudge (OR) theory.[12] These cross sections agree well with Corrigan's experimental electron-impact dissociation cross sections[13] from threshold

* Jet Propulsion Laboratory. Work supported in part by the National Aeronautics and Space Administration, Contract NAS7-100.

† Albert Amos Noyes Laboratory of Chemical Physics, Contribution No. 3705. Work supported in part by the U.S. Atomic Energy Commission. Report Code CALT 532-33.

‡ Present address: The Max Planck Institute for Physics and Astrophysics, Institute for Extraterrestrial Physics, 8046 Munich, Germany.

[1] For a review of early work in this field see H. S. W. Massey and E. H. S. Burhop, *Electronic and Atomic Impact Phenomena* (Oxford University Press, London, 1952).

[2] (a) G. J. Schulz, Phys. Rev. **112**, 150 (1958); (b) G. J. Schulz and J. W. Philbrick, Phys. Rev. Letters **13**, 477 (1964).

[3] (a) E. N. Lassettre, Radiation Res. Suppl. **1**, 530 (1959); (b) A. Skerbele, M. A. Dillon, and E. N. Lassettre, J. Chem. Phys. **46**, 4161 (1967); (c) **46**, 4162 (1967).

[4] (a) A. Kuppermann and L. M. Raff, J. Chem. Phys. **37**, 2497 (1962); (b) **39**, 1607 (1963); (c) Discussions Faraday Soc. **35**, 30 (1963).

[5] (a) F. H. Read and G. L. Whiterod, Proc. Phys. Soc. (London) **82**, 434 (1963); (b) **83**, 619 (1964); (c) **85**, 71 (1965).

[6] (a) H. G. M. Heideman, C. E. Kuyatt, and G. E. Chamberlain, J. Chem. Phys. **44**, 355 (1966); (b) J. A. Simpson, M. G. Menendez, and S. R. Mielczarek, Phys. Rev. **150**, 76 (1966); (c) G. E. Chamberlain, *ibid.* **155**, 46 (1967).

[7] (a) H. Ehrhardt and F. Linder, Z. Naturforsch. **22a**, 11 (1967); (b) H. Ehrhardt and K. Willman, Z. Physik **203**, 1 (1967).

[8] J. P. Doering and A. J. Williams, III, J. Chem. Phys. **47**, 4180 (1967).

[9] (a) J. K. Rice, A. Kuppermann, and S. Trajmar, J. Chem. Phys. **48**, 945 (1968); (b) S. Trajmar, J. K. Rice, P. S. P. Wei, and A. Kuppermann, Chem. Phys. Letters **1**, 703 (1968).

[10] Under investigation in our laboratories.

[11] D. C. Cartwright and A. Kuppermann, Phys. Rev. **163**, 861 (1967).

[12] (a) R. A. Bonham, J. Chem. Phys. **36**, 2360 (1964); (b) V. I. Ochkur, Zh. Eksp. Teor. Fiz. **45**, 734 (1963) [Sov. Phys—JETP **18**, 503 (1964)]; (c) M. R. H. Rudge, Proc. Phys. Soc. (London) **85**, 607 (1965); (d) **86**, 763 (1965); (e) D. S. F. Crothers, *ibid.* **87**, 1003 (1966).

[13] S. J. B. Corrigan, J. Chem. Phys. **43**, 4381 (1965).

to about 50 eV. A comparison between the theoretical and experimental angular distributions as functions of incident energy provides an additional and more sensitive test of the theory, since integration of the differential cross section may conceal a failure of the theory while still leading to the correct total cross section. Green[14] has pointed out that the arguments of Rudge[12c,12d] and Crothers[12e] justifying Rudge's modification of the Ochkur theory are of doubtful validity and the best test of these theories is comparison with experimental differential cross sections. Hence, the (OR) approximation has been used to calculate the differential cross sections for the $X\,^1\Sigma_g^+ \rightarrow b\,^3\Sigma_u^+$ and $X\,^1\Sigma_g^+ \rightarrow a\,^3\Sigma_g^+$ excitations for comparison with the equivalent experimental measurements. The singlet–triplet transition provides an unambiguous test of rearrangement scattering theories since they are due entirely to exchange excitation with no contribution from the direct process.

A broad feature in the electron-impact spectrum of H_2 corresponding to the $X\,^1\Sigma_g^+ \rightarrow b\,^3\Sigma_u^+$ transition has been observed by Schulz[2a] and Dowell and Sharp[15] using the trapped-electron method. By this method the total cross section is measured very near threshold energy. Kuppermann and Raff[4c] also observed the $X\,^1\Sigma_g^+ \rightarrow b\,^3\Sigma_u^+$ transition at 60-eV impact energy with an apparatus which collected scattered electrons from 22° to 112°, the collection efficiency being highest at 90°. To our knowledge there are no experimental or theoretical differential cross sections for electron-exchange processes in molecular hydrogen to which our results can be compared.

II. THEORY

Most previous calculations of the exchange excitation of atoms by low-energy electrons have been performed in the Born–Oppenheimer (BO) approximation.[16] The results of such calculations, however, indicate that the (BO) approximation fails badly for incident electron energies below about 100 eV.[17] The calculation of similar exchange processes involving diatomic molecules has been limited by the mathematical difficulty of treating the noncentral molecular force field and the nuclear motion. Ochkur[12b] and Rudge[12c] have proposed modifications of the (BO) approximation which have been found to give reliable total cross sections for exchange processes in atomic systems. Recently, this (OR) approximation was employed to calculate total cross sections for excitation of the $(b\,^3\Sigma_u^+)$ and $(a\,^3\Sigma_g^+)$ states of molecular hydrogen.[11] The methods used in the cross-section calculations reported here are very similar to the ones used in the total-cross-section calculations and consequently are only briefly outlined.

Within the framework of the (BO) separation of nuclear and electronic motion[18] and the (OR) approximation to the exchange scattering amplitude of an electron by a diatomic molecule, the differential cross section for exchange excitation from initial state $i(n, \nu, J, M)$ to final state $f(n', \nu', J', M')$ can be written as

$$I_i^f(k_0, \theta, \varphi) = \frac{3k'}{k_0}\left|\int_{R,\Omega} \xi^*_{n'\nu'J'}(R)\, Y^*_{J'M'}(\chi, \phi)\, T_i^f \xi_{n\nu J}(R)\, Y_J^M(\chi, \phi) R^2 dR d\Omega\right|^2, \tag{1}$$

where

$$T_i^f(k_0, \theta, \varphi; R, \chi, \phi) \equiv \frac{2a_0}{[a_0 k' - i(I_n/\mathcal{R})^{1/2}]^2}\int \exp(i\mathbf{q}\cdot\mathbf{r}_1)\psi^*_{n'}(\mathbf{r}_1, \mathbf{r}_2; R)\psi_n(\mathbf{r}_1, \mathbf{r}_2; R)\, d\mathbf{r}_1 d\mathbf{r}_2. \tag{2}$$

In Eqs. (1) and (2), ψ, ξ, and Y are the spatial electronic, vibrational and rotational wavefunctions; I_n is the ionization energy of state n; $\mathcal{R}$ is the Rydberg energy; a_0 is the Bohr radius; R is the internuclear distance; χ, ϕ are the polar orientation angles of the internuclear axis with respect to a space-fixed coordinate system; $d\Omega$ is the element of solid angle in the direction of the internuclear axis; θ and φ are polar angles defining the direction of scattering with respect to the direction of the incoming free electron; $\mathbf{r}_1$ and $\mathbf{r}_2$ are the coordinates of the bound electrons in the molecule-fixed coordinate system; n, ν, and J are the electronic, vibrational and rotational quantum numbers; $\mathbf{k}_0$, $\mathbf{k}'$ are the initial and final wavenumber vectors of the free electron which are related by

$$k'(k_0, i, f) = [k_0^2 - (2m/\hbar^2)(E_f - E_i)]^{1/2}, \tag{3}$$

where E_i and E_f represent the total energy of the molecule before and after collision, and finally

$$\mathbf{q} = \mathbf{k}_0 - \mathbf{k}'.$$

The factor of 3 in Eq. (1) comes from integration over spin variables. Since the presently available experimental

[14] T. A. Green, Proc. Phys. Soc. (London) **92**, 1144 (1967).
[15] J. T. Dowell and T. E. Sharp, J. Chem. Phys. **47**, 5068 (1967).
[16] J. R. Oppenheimer, Phys. Rev. **32**, 361 (1928).
[17] D. R. Bates, A. Fundaminsky, J. W. Leech, and H. S. W. Massey, Trans. Roy. Soc. (London) **A243**, 117 (1950).
[18] M. Born and R. Oppenheimer, Ann. Physik **84**, 457 (1927).

energy resolution is not sufficient to resolve rotational transitions, only rotationally averaged differential cross sections will be considered here. If the temperature of molecular hydrogen is appreciably higher than its rotational characteristic temperature (174°K), then the rotationally averaged differential cross section for a gaseous thermal target is given by

$$I_{n\nu}^{n'\nu'}(k_0, \theta, \varphi) = \frac{3k''}{k_0} \int_\Omega \left| \int_R [R\xi_{n'\nu'}(R)]^* T_{n\nu}^{n'\nu'}(k_0, \theta, \varphi; R, \chi, \phi)[R\xi_{n\nu}(R)]dR \right|^2 \frac{d\Omega}{4\pi}, \tag{4}$$

where

$$k''(k_0, n, \nu, n', \nu') = [k_0^2 - (2m/\hbar^2)(E_{n'\nu'} - E_{n\nu})]^{1/2}. \tag{5}$$

In the derivation of (4), the vibrational wavefunctions and the wavenumber of the scattered electron were assumed independent of J and J'. This assumption is consistent with present experimental energy resolution capabilities.

The excited ($b\,^3\Sigma_u^+$) state is unbound and hence there is a continuum of ν'-vibrational states. The differential cross section for excitation to all final vibrational states is formed from (4) by "summing" over ν'. Application of the delta-function approximation[19] to (4) leads to a rotationally averaged differential cross section for excitation from the ground vibrational state to *all* excited vibrational states which is given by

$$I^{(1)}(k_0, \theta, \varphi) = \frac{3k''}{k_0} \int_{D_0}^{E_0} P^{(1)}(E_1) \langle | T_{\nu'}^{(1)} R^{(1)}(E_1) |^2 \rangle dE_1, \tag{6}$$

where

$$P^{(1)}(E_1) \equiv | R^{(1)}(E_1)\xi_0^{(0)}[R^{(1)}(E_1)] |^2 \Big/ \int_{D_0}^{\infty} | R^{(1)}(E_1)\xi_0^{(0)}[R^{(1)}(E_1)] |^2 dE_1. \tag{7}$$

In the above, D_0 is the dissociation energy of the ground electronic state; E_0 is the energy of the incident electron; $\xi_0^{(0)}$ is the lowest vibrational wavefunction of the ground electronic state; and the angle brackets represent an average over all orientations of the internuclear axis with respect to the incident electron beam. The integration over the internuclear distance R has been transformed to an integration over the corresponding potential energy E_1. $E_1(R)$ is the expression for the potential energy of the $b\,^3\Sigma_u^+$ state as a function of internuclear distance and $R^{(1)}(E_1)$ is the inverse of this function.

The $a\,^3\Sigma_g^+$ state is bound (dissociation energy 2.91 eV) and has about 16 vibrational states and no continuum whose left classical turning points fall within the Frank–Condon vertical band from the ground electronic-vibrational state. The calculation of the differential cross section for this state is performed similarly to that of the $b\,^3\Sigma_u^+$ state.

In the calculations reported here, the electronic wavefunctions used were those of Weinbaum[20] for the ground state, Phillipson–Mulliken[21] for the $b\,^3\Sigma_u^+$ state, and a two-parameter Hartree–Fock wavefunction for the $a\,^3\Sigma_g^+$ state. The numerical methods used were similar to those discussed previously[11] and the results reported here are believed to have computation errors of less than 10%.

[19] (a) A. S. Coolidge, H. M. James, and R. D. Present, J. Chem. Phys. **4**, 193 (1936); (b) H. M. James and A. S. Coolidge, Phys. Rev. **55**, 186, (1939).

[20] C. Weinbaum, J. Chem. Phys. **1**, 593 (1933).

[21] P. E. Phillipson and R. S. Mulliken, J. Chem. Phys. **28**, 1248 (1958).

III. MEASUREMENT OF THE CROSS SECTIONS

A. Apparatus

The low-energy electron-impact spectrometer used in these experiments is basically the same type as the one described by Simpson[22] and Kuyatt and Simpson.[23] It consists of a low-energy electron gun, a scattering chamber, two hemispherical electrostatic analyzers (for generating a monochromatic electron beam and energy-analyzing the scattered electrons), and a detector. The resolution of each of the two electrostatic analyzers is variable in the 0.030–0.300-eV energy range by appropriately adjusting the sphere potentials. The scattering chamber is a welded-bellows cylinder, which allows a variation in scattering angle from −30° to +90°. The convolutions of the bellows have an "s" shape and form an electron trap which reduces the effect of wall scattering which could seriously interfere with the measurements at higher angles. The scattering-chamber sample pressure is normally in the 10^{-5}–10^{-2}-torr region. The pressure is measured with miniature ion and thermocouple gauges and is kept constant during an experiment by a variable leak and a pressure controlling system. Temperature control of the target gas is possible by introducing cooling or heating media into the area between the scattering chamber and a second bellows which surrounds it. The second electrostatic energy analyzer is tuned to pass electrons with the same

[22] J. A. Simpson, Rev. Sci. Instr. **35**, 1698 (1964).

[23] C. E. Kuyatt and J. A. Simpson, Rev. Sci. Instr. **38**, 103 (1967).

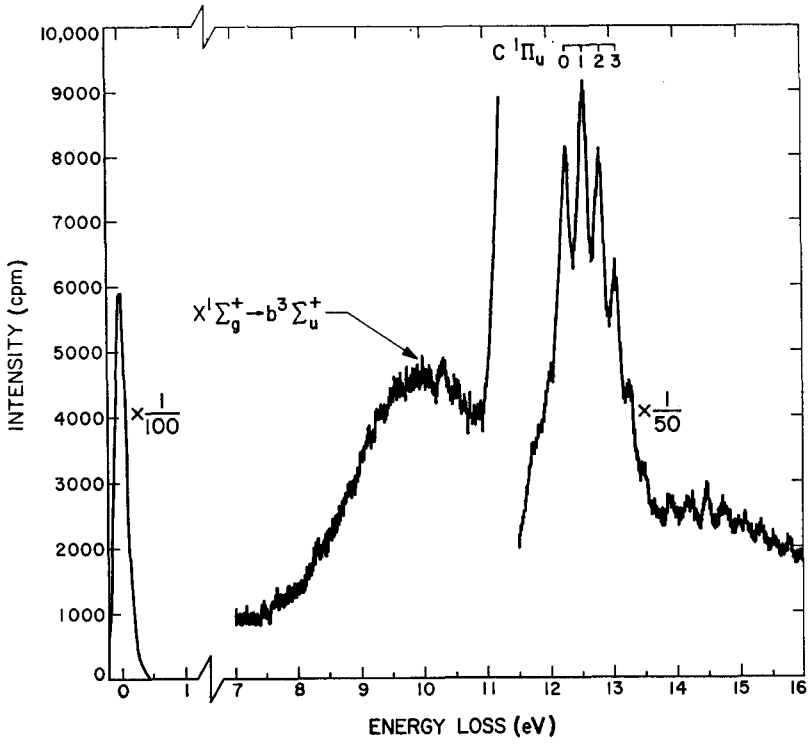

FIG. 1. Electron-impact energy-loss spectrum of molecular hydrogen at 50-eV impact energy and 40° scattering angle. Ion gauge reading (uncalibrated): 2×10^{-3} torr. Incident beam current: 2.8×10^{-8} A. Elastic peak FWHM: 0.22 eV.

energy as the first energy selector. A sweep voltage is applied between scattering chamber and center of the second analyzer. When this voltage is zero, electrons that did not lose any energy during the scattering will pass this analyzer and reach the detector, a 20-stage electron multiplier. The multiplier output can be coupled to a count rate meter or a 1024 channel scaler. As the sweep voltage is gradually increased, electrons that have lost the corresponding energy in exciting the molecular target will reach the detector. The number of electrons counted per unit time versus the sweep voltage furnishes an energy-loss spectrum. The energy-loss sweep voltage is controlled either by a sweep generator or by the multichannel scaler whose memory channel number (into which counting occurs) is converted to an analog voltage. External field effects are eliminated with appropriate radio frequency and magnetic shielding. The entire apparatus is bakeable to 400°C. A more detailed description of the system is given elsewhere.[24]

B. Experimental

In these experiments the electron current scattered into a given solid angle of approximately 10^{-3} steradian was measured as a function of energy loss at a fixed electron-impact energy. A typical energy-loss spectrum is shown in Fig. 1. It is an X–Y recording of the count-rate-meter output. The X axis represents the energy loss of the electrons and the Y axis corresponds to the number of electrons per min reaching the detector with each particular energy loss. This spectrum was obtained with an electron-impact energy of 50 eV and a scattering angle of 40°. The elastic peak shown on the left-hand side determines the zero energy loss point.

The apparatus for the $b\ ^3\Sigma_u^+$ excitation was tuned to about 0.2 eV resolution (full width at half-maximum FWHM of the elastic peak). This was a reasonable choice to insure high signal level and partial resolution of the vibrational structure of the $X\ ^1\Sigma_g^+ \rightarrow C\ ^1\Pi_u$ transition. Most of the measurements were made with a count rate meter with a time constant that varied from 0.5 sec for the elastic peak to 10 sec for the triplet transition at high angles. The energy-loss sweep rate was adjusted accordingly to give an undistorted reproduction of the features. The energy-loss scale is absolute being measured with a digital voltmeter with respect to the center of the elastic peak. Its accuracy (about 10 mV) is verified by the optical values of the portions of the vibrational bands of the $C\ ^1\Pi_u$ excitation.

For the experiments in the 11–14-eV energy-loss region the instrument was retuned to obtain an over-all resolution of about 0.040 eV (FWHM). Typical spectra at this resolution are shown on Figs. 2 and 3 and discussed below.

In order to monitor the conditions at different angles during the experiment, and check the over-all instrument stability, the pressure and the beam current in the scattering chamber were measured and the elastic peak

[24] S. Trajmar, J. K. Rice, and A. Kuppermann, JPL Tech. Memo, No. 33-373.

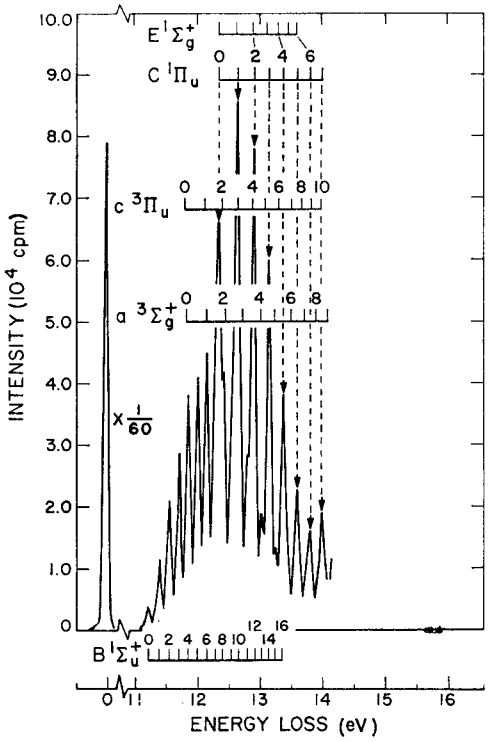

FIG. 2. Electron-impact spectrum of H_2 in the 11–14-eV energy-loss range at 40-eV impact energy and 20° scattering angle. Incident beam current: 1.0×10^{-8} A. Elastic peak FWHM: 0.040 eV.

was scanned before and after each energy-loss spectrum was taken. The pressure of H_2 was kept constant (to within about 5%) at a value between 1 and 2 μ during each experiment and the linearity of the scattered current with pressure was established from 0.1 μ up to 2 μ.

C. Scattering Volume Correction and Error Estimation

Measurements taken at different scattering angles correspond to different scattering geometry. If one wants to compare cross sections at different angles, a normalization of all measurements to the same scattering geometry is necessary. It is customary[25] to carry out this normalization by multiplying the scattered current by $\sin\theta$, where θ is the scattering angle. This procedure yields proper normalization only if the electron beams entering the scattering chamber and the electron optics of the detector system have small diameter and angular divergence.

In our instrument, circular apertures are used for collimating and focusing the electron beam. The scattering geometry is shown on Fig. 4. Both the electron beam entering the scattering chamber and the directions viewed by the electron optics at the exit of this chamber are represented by cones. Typical values for the incident beam and exit viewing cone half-angles are 3° and 4.5°, respectively. The intersection of these two cones defines the volume from which scattered particles can reach the detector. The solid angle extended by the detector varies from point to point within this volume; in fact, it drops to zero at the extremes. One has to average, therefore, the solid angle over this volume to get an effective value of (scattering length) $\times$ (solid angle) $\equiv (ld\Omega)_{\text{eff}}$. This problem has been discussed by Breit, Thaxton, and Eisenbud,[26a] and by Critchfield and Dodder.[26b] Every differential volume element within this volume has to be properly weighted for electron density and solid angle subtended at the entrance of the detector optics. For normalizing our measurements, the incoming beam was considered as a cone with a truncated Gaussian electron density distribution having its maximum along the cone axis. The density-weighted volume elements of the beam cone were integrated within the limits defined by the surface of the view cone. Each element was also weighted by the inverse square of the distance from the entrance aperture of the detector to allow for the solid angle of the detector at the volume element. The value of $(ld\Omega)_{\text{eff}}$ at each angle was normalized to the value at 90°. At $\theta=10°$, the difference between these calculations and the approximate $\sin\theta$ correction is about 10%. The differential scattering cross section for a particular excitation is proportional to the peak height (after correction for scattering geometry) provided that the cross section is independent of angle within the range defined by the view cone and that the line shape is independent of angle.

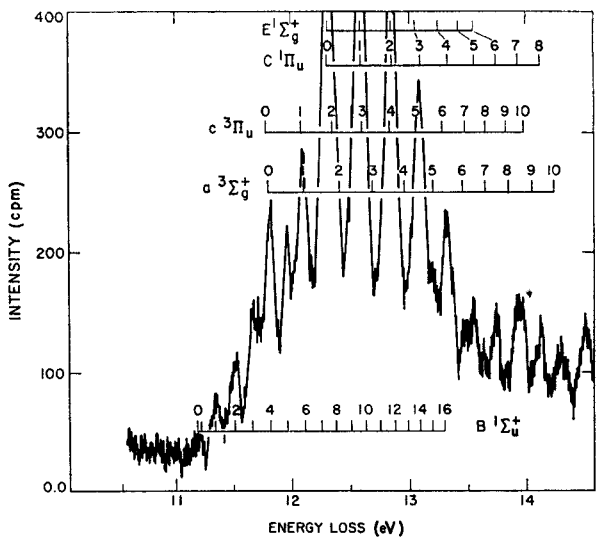

FIG. 3. Electron-impact spectrum of H_2 in the 11–14-eV energy-loss region at 80° scattering angle. The experimental conditions are the same as for Fig. 2.

[25] L. Vriens, J. A. Simpson, and S. R. Mielczarek, Phys. Rev. 165, 7 (1968).

[26] (a) G. Breit, H. M. Thaxton, and L. Eisenbud, Phys. Rev. 55, 1018 (1939); (b) C. L. Crithfield and D. C. Dodder, *ibid.* 75, 419 (1949).

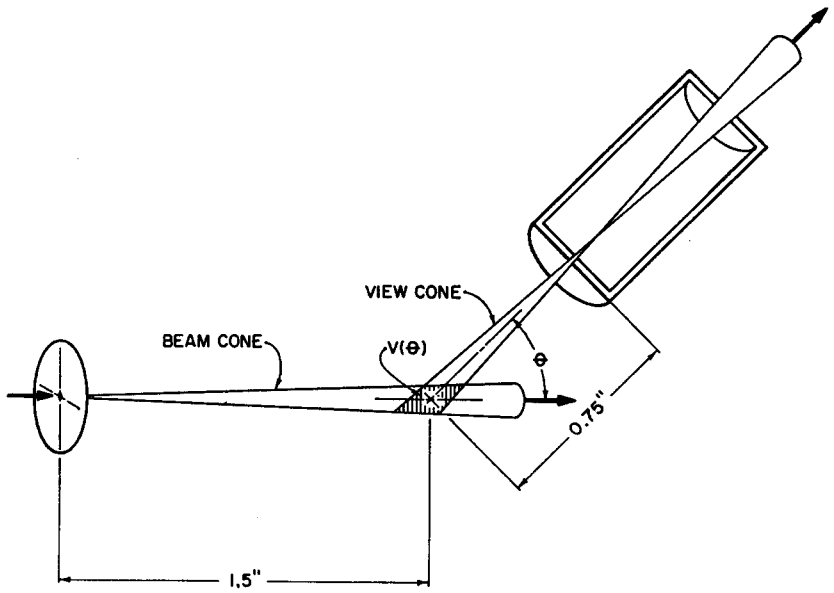

FIG. 4. The scattering geometry showing the target volume and the beam and view cones.

The errors inherent in the reduced measurements are of three types:

(1) *Random fluctuations and background noise*: If the number of counts per second reaching the detector is N, then from the statistical nature of the counting process, the uncertainty in N (one standard deviation) is $\pm(N/\tau)^{1/2}$, where τ is the time constant (in seconds) of the rate meter.[27] This fluctuation was always less than 5% for the $X\,^1\Sigma_g^+ \rightarrow b\,^3\Sigma_u^+$ peak. In addition, there is a background noise due to stray electrons, electronic noise, and cosmic rays. This noise is relatively independent of scattering angle and amounts to about 2 counts/sec.

(2) *Effective scattering volume correction*: Another source of error arising from the effective volume correction is due to the $\pm 1°$ uncertainty in the scattering angle and the uncertainties in the beam and view cone angles. These latter angles cannot be determined directly with the present experimental setup. The last, however, can be estimated from the electron optics with satisfactory accuracy. The beam cone angle is then obtained from the direct beam intensity profile as measured on the first dynode of the multiplier as a function of scattering angle. (The peak position of this curve defines the zero scattering angle.)

(3) *Instrumental error*: This includes all effects associated with the variation of pressure, beam intensity, and over-all instrument detection efficiency during the measurements. The constancy of these quantities is monitored during each energy-loss sweep but a significant change of instrument detection efficiency with scattering angle could go undetected. The fact that the optimum tuning conditions are found to be the same at any angle and that the scattering intensity is symmetric around zero angle indicates that this effect is negligible.

The error bars assigned to the measurements include estimated contributions from these three sources of error.

IV. RESULTS AND DISCUSSION

As seen in Fig. 1, the inelastic feature corresponding to the $X\,^1\Sigma_g^+ \rightarrow b\,^3\Sigma_u^+$ transition has a maximum at about 10 eV energy loss. Since the $b\,^3\Sigma_u^+$ state of H_2 is unstable with respect to dissociation into two hydrogen atoms, the transition is represented by a broad feature whose shape seems to be determined[11] by the Frank–Condon overlap integrals.[28a] In the 11–14-eV energy-loss region several singlet and triplet transitions overlap.[28b] The optical vibrational band progression for the $X\,^1\Sigma_g^+ \rightarrow C\,^1\Pi$ transition is shown.

To determine the angular dependence of the differential cross section for this transition, the corresponding maximum ordinate was read off the energy-loss spectrum at each angle and normalized to the same scattering volume with the calculated effective scattering volume described above. Using this peak height instead of the area under the band does not introduce any error if the line shape is the same at all angles. We found that this was indeed the case for both the elastic and inelastic features of the energy-loss spectra. In order to compare the absolute theoretical and relative experimental cross sections, the latter are multiplied at each energy by a factor which is the average of the ratios of the calculated absolute and experimental relative cross sections at each angle. The possibility of appreciable contribu-

[27] R. D. Evans, *The Atomic Nucleus* (McGraw-Hill Book Co., New York, 1955), p. 807.

[28] (a) G. Herzberg, *Spectra of Diatomic Molecules* (D. Van Nostrand Co., Princeton, N.J., 1953), 2nd ed., p. 387; (b) p. 530.

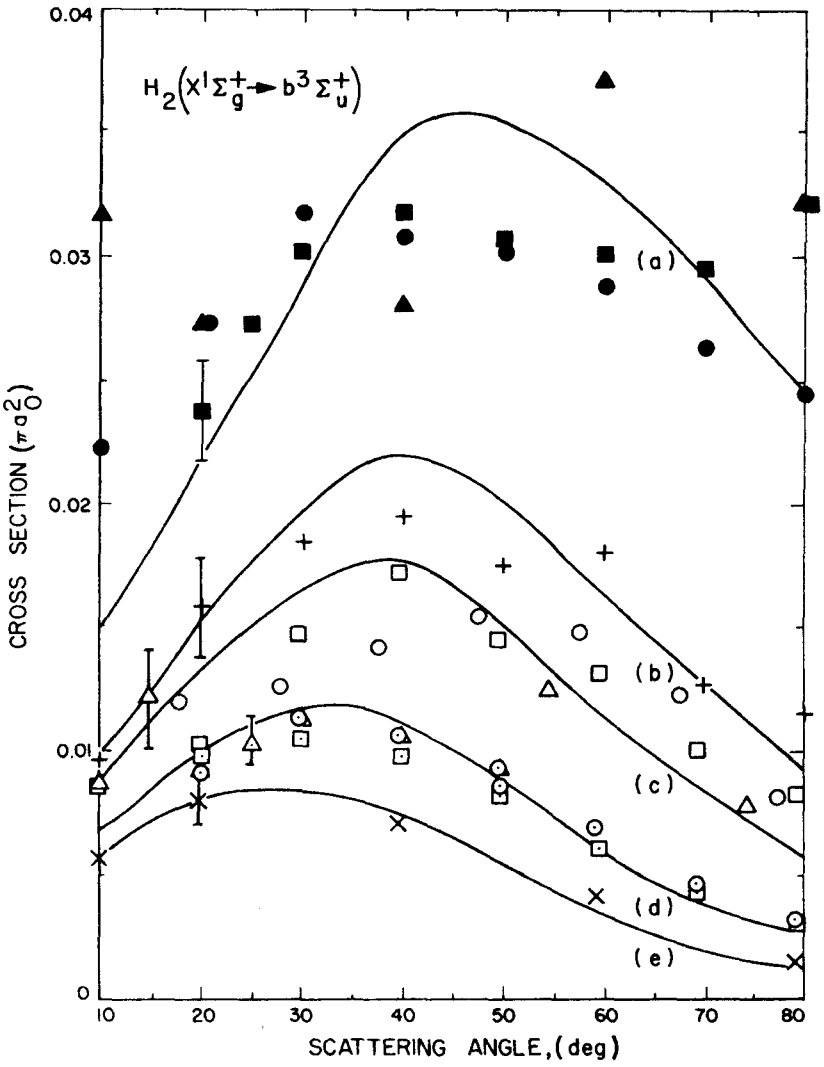

FIG. 5. Differential cross section of $X\ ^1\Sigma_g^+ \rightarrow b\ ^3\Sigma_u^+$ transition in H_2 as a function of scattering angle. Solid curves are theoretical and points are experimental. Different symbols indicate different experiments, conducted over a period of 7 months. Incident energies are (a) 25 eV: ●, ■, ▲; (b) 35 eV: +; (c) 40 eV: ○, □, △; (d) 50 eV: ⊙, ⊡, ⧋; (e) 60 eV: ×.

tion from the strong $C\ ^1\Pi_u$ tail was eliminated by plotting the cross sections obtained not only from the maximum ordinate measurements, but from measurements at 0.5 and 1.0 eV away from that maximum. No change in the shape of the curves of relative cross section versus scattering angle was observed.

Figure 5 compares the theoretical and experimental differential cross sections at 25-, 35-, 40-, 50-, and 60-eV impact energies. The solid curves are the calculated ones. Each experimental point was obtained from a spectrum similar to the one shown in Fig. 1.

At 50 and 60 eV the calculated and observed curves agree quite well. As one goes to lower impact energies, however, the disagreement between theory and experiment increases. While the theory predicts well-formed maxima at around 40° for low impact energies, the experiment shows fairly isotropic scattering below 35 eV. Although the measured differential cross sections are in arbitrary units, the absolute values obtained from them by the procedure described above should be close to the correct ones at 50- and 60-eV impact energies, since for them the experimental and calculated differential cross sections agree very well and the total cross section obtained from the integration of the calculated differential cross sections agrees approximately with Corrigan's measurement.[11,13] In calculating the total cross section, Cartwright and Kuppermann[11] neglected the contribution from the excitation to the $c\ ^3\Pi_u$ state. Inclusion of this contribution may improve this agreement.

The validity of the Ochkur (O) and (OR) theories of electron exchange scattering can be tested only in a very few cases due to the lack of experimental data and/or more accurate theoretical calculations. The (O) approximation may be considered as an (OR) approximation with improper normalization of the wavefunction. For the 2^3S excitation of He, the shape of the experimental differential cross section of Ehrhardt and

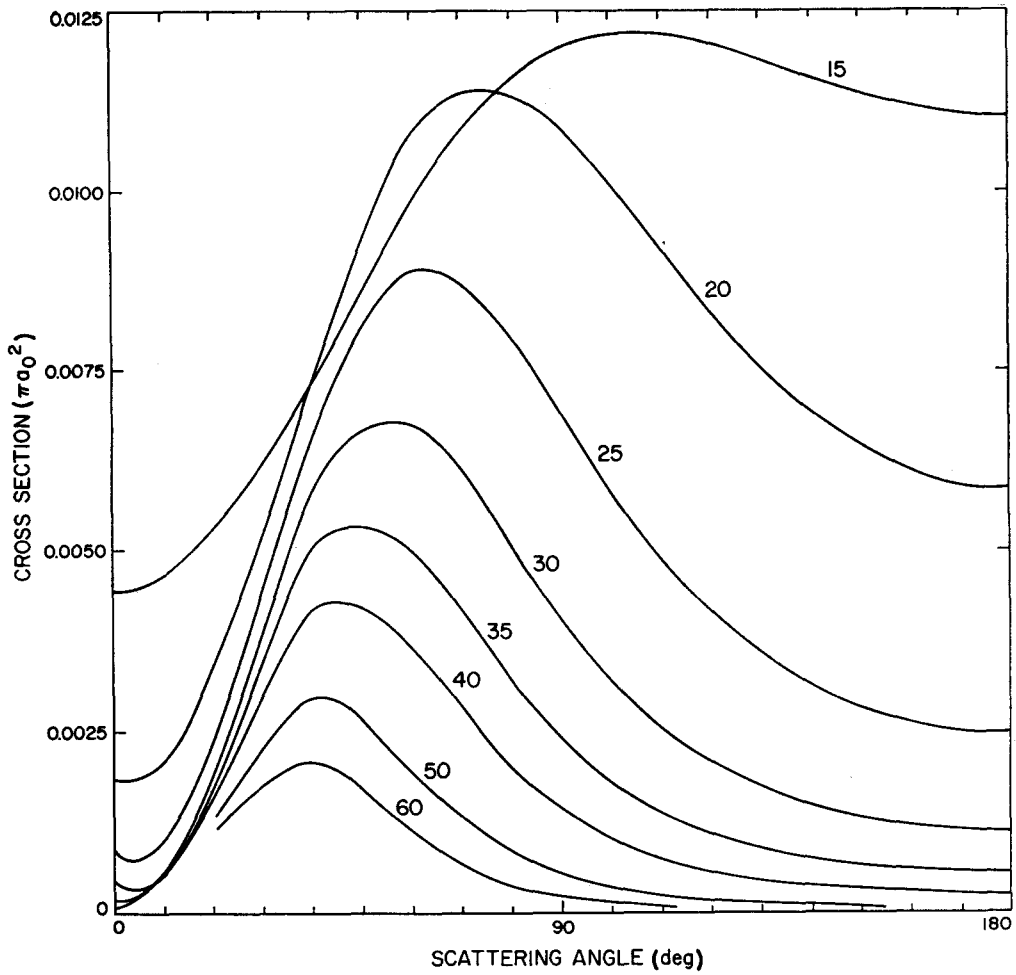

FIG. 6. Differential cross sections calculated for the $X\ ^1\Sigma_g^+ \rightarrow a\ ^3\Sigma_g^+$ excitation. The numbers over the curves represent the electron-impact energy in eV.

Willman[7b] agrees with the OR predictions at 24 eV from 20° to 120°.[29] The experimental data of Simpson, Menderez, and Mielczarek[6b] at 56.5 eV (5°–50°) and of Vriens, Simpson, and Mielczarek[25] in the 100–225-eV energy range (5°–15°) are in complete disagreement with the (OR) and (O) curves for the same excitation. In the case of atomic hydrogen, a comparison of the (OR) differential exchange cross sections for elastic scattering and the $1s \rightarrow 2s$ excitation to the accurate close coupling calculation of Burke, Shey, and Smith[30] has been made by Truhlar, Cartwright, and Kuppermann.[31] They find that the (OR) angular distributions are in qualitative agreement with the close coupling results at intermediate energies but at low energies the agreement is very poor.

It is somewhat surprising, especially in light of the above discrepancies, that the (OR) approximation predicts as well as it does the shape of the angular distribution for the $X\ ^1\Sigma_g^+ \rightarrow b\ ^3\Sigma_u^+$ transition in H_2 for energies as low as 40 eV. Since the theory is based on first-order perturbation principles, the above comparison between theory and experiment implies that for the angular regions and impact energies considered here the deviation of the interactions from first order is not important or that the agreement is simply an accident. It is important therefore to do additional comparisons between experiment and theory before the usefulness of the (OR) approximation can be determined.

Figures 2 and 3 show the energy-loss spectrum of H_2 in the 11–14-eV region with a resolution (FWHM) of about 0.040 eV at 20° and 80°, respectively. The electron-impact energy was 40 eV for these experiments. Many of the vibrational features of the $B\ ^1\Sigma_u^+$ and $C\ ^1\Pi_u$ excitation are separated and they account practically for all the intensity at 20°. At higher angles, however, contribution to the inelastic scattering from

[29] D. C. Cartwright, thesis, California Institute of Technology, Pasadena, California, June 1967, (unpublished).

[30] (a) P. G. Burke, H. M. Schey, Phys. Rev. **126**, 147 (1962); (b) P. G. Burke, H. M. Schey, and K. Smith, Ibid. **129**, 1256 (1963).

[31] D. C. Truhlar, D. C. Cartwright, and A. Kuppermann, Phys. Rev. **175**, 113 (1968).

the $a\,^3\Sigma_g^+$ and/or $c\,^3\Pi_u$ state is definitely observable. The intensity envelope of the $B\,^1\Sigma_u^+$ vibrational bands is easily recognized on Fig. 2. The intensity of consecutive vibrational features follows this envelope smoothly. At 80°, however, the bands with $\nu'=4$ and 6 are much more intense than they should be according to this intensity envelope. The extra intensity comes from the contribution of the $\nu'=0$ and 1 bands of the $a\,^3\Sigma_g^+$ and/or $c\,^3\Pi_u$ excitations. Dowell and Sharp[15] argue that in their electron-trap threshold spectra the dominant features in H_2 are associated with the $c\,^3\Pi_u$ excitation and that all other contributions are negligible. It is not possible to tell from our spectra whether the $a\,^3\Sigma_u^+$ or $c\,^3\Pi_u$ scattering is responsible for the intensity enhancement we observe. At 40 eV electron energy the singlet bands are stronger than the triplet ones even at high angles and their interference prohibits a definite conclusion. It would require a much better resolution to separate the $a\,^3\Sigma_u^+$ and $c\,^3\Pi_u$ features from the overlapping singlet ones.

The differential cross sections calculated for the $X\,^1\Sigma_g^+ \rightarrow a\,^3\Sigma_g^+$ excitation are shown in Fig. 6. No experimental data are available for comparison, for the reasons just given.

ACKNOWLEDGMENTS

The authors are grateful to Dr. J. A. Simpson and Dr. C. E. Kuyatt for valuable advice concerning the design of the instrument and to Mr. G. Steffensen for his help in carrying out the measurements. They would also like to acknowledge helpful discussions with Professor R. M. Pitzer and Professor W. A. Goddard, and Mr. D. G. Truhlar of the California Institute of Technology, concerning certain aspects of the theoretical work.

THE JOURNAL OF CHEMICAL PHYSICS VOLUME 49, NUMBER 12 15 DECEMBER 1968

Shock-Tube Study of Vibrational Exchange in N_2–O_2 Mixtures

D. R. WHITE

General Physics Laboratory, General Electric Research and Development Center, Schenectady, New York 12301

(Received 7 August 1968)

Vibrational excitation in gas mixtures can occur both by translation-to-vibration (T–V) energy conversion in simple collisions and by the exchange of vibrational energy (V–V) between components. Nitrogen–oxygen mixtures containing 5%, 10%, 21%, 33%, and 50% O_2 have been studied in a shock tube using both optical interferometry to measure the density profile through the relaxation zone and infrared emission of CO added in small quantities to serve as an indicator of the degree of vibrational excitation of N_2. The density increase has been resolved into the sum of short and long time-constant exponentials. The former is approximately that expected from excitation of the O_2 component. The longer time constant of the increasing density is approximately that observed for the infrared emission of CO and is thus indentified with the N_2 excitation. This latter is found to be more rapid than can be accounted for by a T–V process and therefore vibrational exchange with excited O_2 must contribute signficantly. Data have been analyzed to obtain a transition probability per collision for the exchange process which varies from 10^{-6} to 2.3×10^{-5} over the range 1000°–3000°K.

INTRODUCTION

The translation–rotation shock front in a diatomic gas is followed by a relatively long region in which the vibrational energy content of the gas increases from its initial pre-shock value to that value corresponding to thermal equilibrium. This conversion of energy from translation to internal degrees of freedom may take place in at least two ways. If only one diatomic species is present, a simple translation-to-vibration (T–V) energy conversion process is operative, i.e., for each vibrational quantum generated in a collision, that amount of kinetic energy has disappeared. Exchange of a quantum between like molecules has no thermodynamic significance. When two diatomic species are present, the appearance of a quantum of energy in one may be marked by the disappearance of a quantum from the other, with the energy difference being supplied from (or going to) the kinetic energy of the colliding molecules. This is termed a vibration-to-vibration (V–V) energy transfer process. We shall not consider systems in which rotational energy is known to be important.

The former T–V process has been studied intensively, and the excitation of simple systems is relatively well understood, where a simple system is considered as one in which a non-hydrogen-containing diatomic molecule is vibrationally excited in collision with a monatomic or a ground-vibrational-state diatomic molecule. Much of the data prior to 1963 are referenced and correlated in Ref. 1. Additional shock-tube data on N_2 and O_2

[1] R. C. Millikan and D. R. White, J. Chem. Phys. 39, 3209 (1963).